 Water Supply | in press | 2021

Application of numerical modeling to reservoir immersion assessment and control in dual-formation hydrogeological unit

Yun Yang, Wengui Nan, Shenggen Guo, Dan Jin, Jianhui Wu, Yu Zhang, Zhi Dou and Zhifang Zhou

ABSTRACT

Reservoir immersion is a serious environmental geological issue in a dual-formation structural reservoir bank (DFB) induced by dynamic surface water impoundment (SWI) that has implications for low-lying farmland and buried infrastructure. It is a major challenge to identify the dynamic immersion process and make economic and scientific joint mitigation measures for controlling groundwater immersion. Here, we develop a three-dimensional groundwater flow model and apply it to evaluate and control reservoir immersion in the typical low-lying DFB of Xingan Navigation and Power Junction Project (XGNPJ) across Ganjiang River in Jiangxi Province, China. The field-scale model is well calibrated to predict where the groundwater immersion could potentially occur. Furthermore, the effectiveness of the countermeasures adopted for the reduction of reservoir immersion areas were analysed based on the simulation model by considering the projected future combination scenarios of engineering measures. Results indicate that without engineering mitigation measures, SWI generates groundwater inundation across 23% of the total study area. Comprehensive comparative analysis on different seepage control schemes reveals that the joint engineering measures can effectively control the immersion range to 5% of the total area. The findings can provide scientific basis for groundwater immersion assessment and guide immersion control of XGNPJ project.

Key words | cut-off wall, dual-formation structure, groundwater modeling, relief well, reservoir immersion, surface water impoundment

Yun Yang (corresponding author)
Wengui Nan
Yu Zhang
Zhi Dou
Zhifang Zhou
School of Earth Sciences and Engineering,
Hohai University,
Nanjing 210098,
China
E-mail: *yy_hhu@hhu.edu.cn*

Shenggen Guo
Jianhui Wu
Xingan Navigation and Power Junction Construction Management Office of Jiangxi Provincial Port and Waterway Construction Investment Co.,
Nanchang 330038,
China

Dan Jin
China Water Resources Pearl River Planning Surveying and Designing Co. Ltd.,
Guangzhou 510610,
China

HIGHLIGHTS

- Hydrological analysis related to the groundwater-surface water interactions.
- Impacts of groundwater depth on reservior immersion.
- Establishing a FEFLOW model for regional groundwater assessment and identification of the dynamic immersion process.
- Implementation of model assessment for controlling groundwater immersion.
- The joint engineering measures can effectively control the immersion range.

INTRODUCTION

Over the past three decades, massive water conservancy projects in the form of navigation and hydropower junction

doi: 10.2166/ws.2021.050

have been constructed in China to bring tremendous benefits in flood control, water scarcity alleviation, and clean energy generation (Liu *et al.* 2013; Jia 2016). However, water conservancy development has caused serious groundwater immersion due to surface water impoundment (SWI) in the dual-formulation structural reservoir bank (DFB) (Azamathulla *et al.* 2008; Qin & Zhang 2010; Luo *et al.* 2012; Chen *et al.* 2018; Guo *et al.* 2019). As shown in Figure 1, the rise of river level will advance the lateral infiltration from surface water to the lower coarse-grained layer, and the subsequent vertical discharge to the upper fine-grained layer, producing groundwater inundation resulting from narrowing and loss of the vertical unsaturated subsurface space (Habel *et al.* 2017). Further development of immersion issues will cause soil degradation hazards, engineering geological disasters on the foundations of infrastructures, which will seriously affect the local industrial and agricultural production and the stability of the residents in the upper reaches of the reservoir (Fowler & Maddox 1974; Dos Santos *et al.* 2004; Yan *et al.* 2004; Li *et al.* 2018). Therefore, it is significant to identify the dynamic immersion process and make economic and scientific combination of mitigation measures for controlling reservoir immersion after the long-term operation of SWI.

The analytical method with numerical simulation approach is often applied to evaluate reservoir immersion in a plain reservoir with a dual-formation structure (Mahdavi 2015; Hu *et al.* 2015). During early engineering planning, the evaluation of the immersion area is usually through a prediction method recommended by the Kaminski formula (КАМЕНСКИЙ 1995). However, many scholars have found that the immersion range obtained by the Kaminski method using a simplified calculation model is much larger when applied to a DFB where the permeability coefficient of the lower main aquifer is 2–3 orders of magnitude larger than that of the upper weak aquifer (Hu *et al.* 2015). As a consequence, the Kaminski formula can be improved by being combined with a groundwater hydrodynamic method for application in the evaluation of reservoir immersion under different geological structures and impoundment conditions (Cao *et al.* 2009; Xin *et al.* 2020). Since 2000, with the improvements in computing technology, numerical simulation has become a widely used method to predict the process of immersion under complex hydrogeological conditions, using approaches such as the analytic element (Wu *et al.* 2001), finite difference (Shu & Chen 2002; Luo *et al.* 2012) and finite element methods (Wang *et al.* 2008; Li *et al.* 2018; Liu *et al.* 2018). The analytical and numerical methods both have specific advantages and disadvantages. While the analytical formula is easy to apply in engineering, the conditions under which it is applicable are limited, and cannot describe the complex and transient groundwater flow system. However, the three-dimensional (3D) numerical model can reflect the groundwater flow dynamics in complicated hydrogeological conditions more realistically with high simulation accuracy based on large amounts of basic data and observation data. Given the aforementioned considerations, the dynamic changes in groundwater levels in the left bank of the Ganjiang River were simulated based on the Finite Element subsurface flow system (FEFLOW), under the impoundment condition of the Xingan Navigation and Power Junction Project (XGNPJ). The process of dynamic immersion of groundwater along

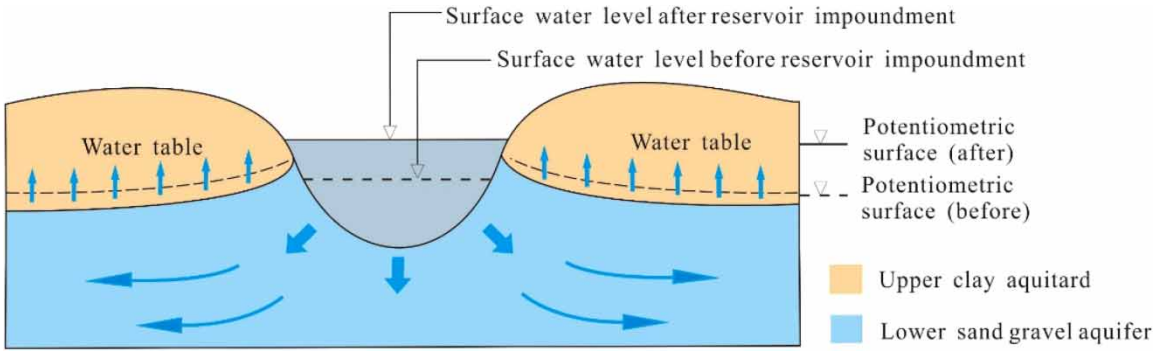

Figure 1 | Schematic diagram of immersion process in dual-formation structural reservoir bank.

the bank with a dual-formation reservoir structure was evaluated, and the range of immersion and degree of immersion hazard in the study area were predicted, thereby providing a scientific basis for the layout of the immersion control scheme in the early stage of the project.

Water conservancy designers and local state government recognize that ongoing SWI will necessitate the development of adaptive design standards with regard to engineering mitigation measures (Wang & Liu 2011; Habel *et al.* 2017). Common engineering measures to control reservoir immersion include cutoff walls (Wang & Liu 2011; Chen *et al.* 2016), relief wells (Li *et al.* 2018; Liu *et al.* 2018) and land lifting reclamation (Hao *et al.* 2011), which can effectively slow down or block the discharge of reservoir water to groundwater in the riparian zone, rapidly reduce the water table around the relief wells and lessen the risk of immersion in low-lying areas along the reservoir bank to facilitate farming and municipal engineering activities, respectively. Adopting economic and scientific combination of mitigation measures is judicious. Therefore, this study designs a variety of joint immersion control engineering measures based on a regional numerical transient groundwater flow model. The current study optimized the affordability and efficiency of the control scheme by comparing and analyzing the effect of immersion control, thereby providing technical support for the application of a seepage control scheme in the early stage of impoundment in the Xingan navigation power junction project.

STUDY AREA: RESERVOIR AREA OF XGNPJ

Background

XGNPJ is located in the end section of the middle reaches of Ganjiang River, about 20 km north of Xingan City, Jiangxi Province, China (Figure 2). The Ganjiang River is the largest river in Jiangxi Province, flowing from south to north and finally importing into Poyang Lake, which is one of the most critical ecoregions characterized by irreplaceable environmental and ecological functions (Yin *et al.* 2018). The main function of XGNPJ is navigation and power generation with a normal storage level of 32.5 m, about 2.0 m higher than the average annual water level of Ganjiang River.

Reservoir immersion is a serious geo-environmental issue for agriculture and building structures in plains areas along Ganjiang River. Taking Shihutang Navigation and Power Junction Project as an example, an adjacent reservoir project in the upstream of XGNPJ in Ganjiang River, the immersion happened after one year of reservoir impoundment (Yin & Lu 2015). The groundwater level rose and exceeded the critical immersed groundwater depth, even creating water logging

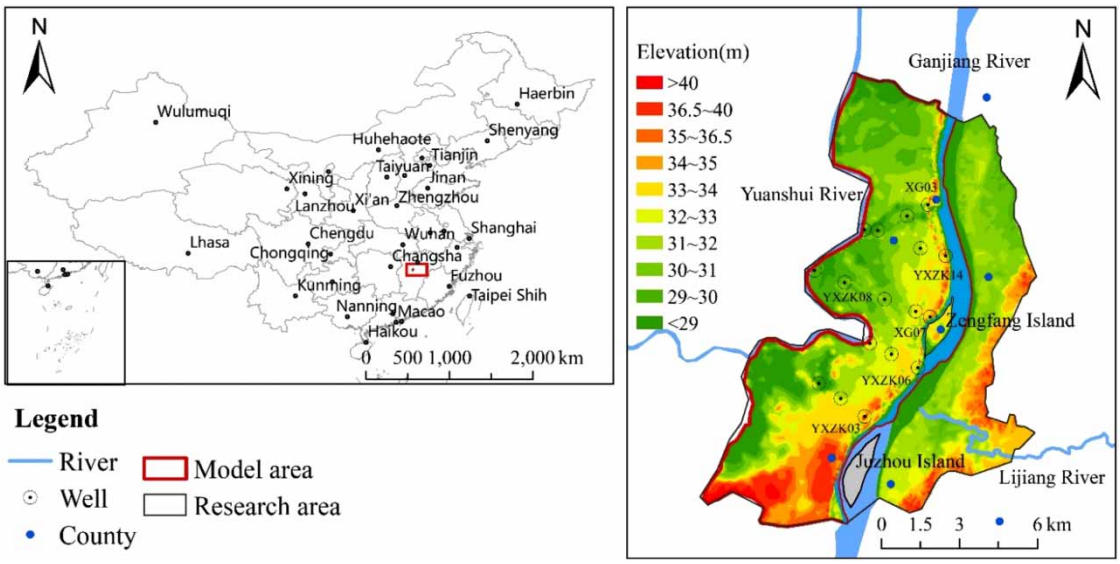

Figure 2 | The geographical extent, topography, surface water system, and hydrogeological borehole in reservoir area of XGNPJ. The red line denotes the boundary of model area.

in the surrounding residential and agricultural cultivated land, especially in areas where the ground elevation is lower than the impounded water level of 56.5 m. In the recent three years, the process of groundwater immersion has been effectively controlled as the result of engineering management measures such as establishment of relief wells, a ditch drainage network system, lifting low-lying fields and so on, spending tremendous financial and material resources. Impounding and operation of XGNPJ will inevitably produce immersion issues in the reservoir area where the topographic and hydrogeological conditions are extremely similar to Shihutang reservoir region. To avoid socio-economic losses caused by immersion disaster, it is essential to identify the dynamic immersion process, evaluate the immersion range, and then optimize the combination of mitigation measures for controlling immersion.

Site description

The left reservoir bank is selected as the research area for several reasons: (1) the left bank region is a closed and independent hydrogeologic unit between Ganjiang River and Yuan River, and is predicted to be threatened by a relatively high degree of reservoir immersion (18 km^2) by steady state analytical equation; (2) the left bank is rich in agricultural resources and intensive socioeconomic activities and it is thus urgent to conduct scientific assessment and control for reservoir immersion; (3) an enormous amount of different types of hydrological and hydrogeological data (from the Geological Survey; Geological Data Information Network of Jiangxi Province, http://www.jxgtt.gov.cn/dzzlg/Index.shtml; National Meteorological Information Center, http://www.nmic.cn/web/index.htm) has allowed us to establish a three-dimensional groundwater model to evaluate the processes in the alluvial groundwater system.

Meteorological and hydrological conditions

The study area receives annual mean precipitation of 1,600 mm and loses about 1,044 mm through surface evaporation per year (1960–2014 average; National Meteorological Information Center), with distinct seasonal variations, creating a humid environment (Zhang *et al.* 2017). In general, annual precipitation consists of dense rain in the rainy season from April to August, accounting for 74% of the total, and a small fraction from September to the next March. The variation of surface water level in Ganjiang station (from http://jasw4.jassw.cn/ja/jaz12.aspx) and groundwater level in two monitoring wells of XG03 and XG07 shows a fairly consistent increase and decrease during the period from 2006/1/1 to 2010/1/1 (Figure 3), which indicates a very close hydraulic connection between surface water and groundwater.

Hydrogeological conditions

The left bank of XGNPJ can be considered to be a relatively independent hydrogeological unit covering 83.9 km^2. The

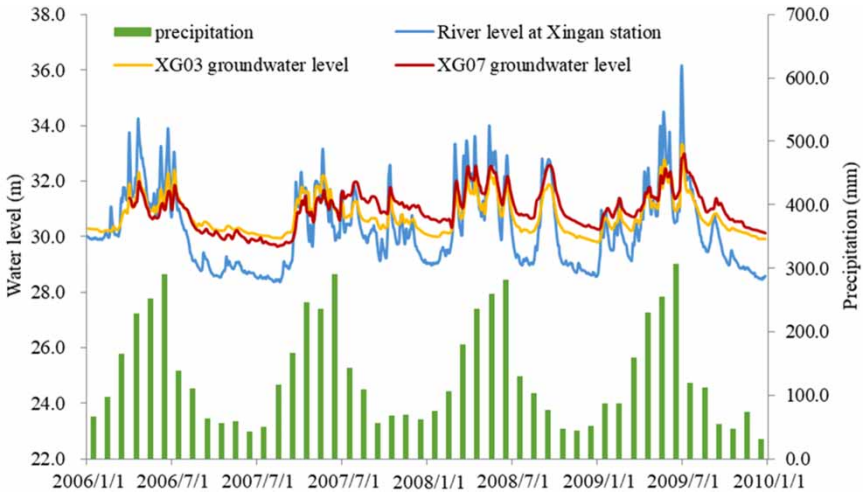

Figure 3 | Variation in precipitation, surface water level in Xingan station, and groundwater level in XG03 and XG07 monitoring wells during the period from 2006/1/1 to 2010/1/1.

regional boundaries of the study area follow the edges of Ganjiang River (east) and Yuan River (west). The study area has typical characteristics of a dual-formation structure. Principal surficial geological units within the study area include the Holocene and upper Pleistocene unit, mainly made of fluvial facies alluvium of the Quaternary age. The Holocene and upper Pleistocene unit comprises two distinct sedimentary formations. The upper layer of this geologic formation is the sandy silt clay, mainly distributed in the surface of the fluvial-deltas plain and the underlying layer is coarse sand and gravel, comprising the alluvial aquifer, which is the principal aquifer in the study area. The aquifer has a high productivity with a potential yield of greater than 16,000 m^3/day with an average thickness of 11 m. The older geological units are the red clastic rock formation in Tertiary and Cretaceous underlying the alluvial aquifer and forming the no-flow bottom boundary. The hydrogeological plane and M-N profile (Figure 4) was mapped by combining multiple data sets from the Geological Data Information Network of Jiangxi Province (http://www.jxgtt.gov.cn/dzzlg/Index.shtml) and the geological survey (2016–2017) conducted by China Water Resources Pearl River Planning Surveying & Designing Co. Ltd.

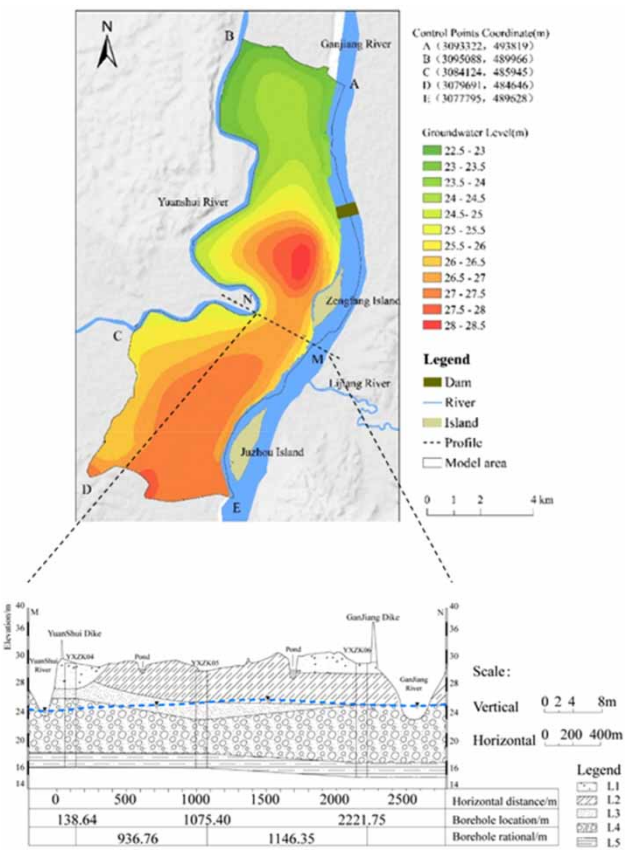

Figure 4 | Hydrogeological conditions of model area showing the plane view and stratigraphic section M-N.

In this region, the Ganjiang River is deeply downcut with an average river-bed elevation of 23–27 m above sea level based on the SRTM 30 m DEM Digital Elevation Database (SRTM Data https://srtm.csi.cgiar.org/srtmdata/). In addition, high linear correlation coefficients (R_{SG}) were determined between groundwater level and nearby surface water level based on the synchronously observed data from groundwater and surface water monitoring (1986–1988) (Guo & Chen 2008). The average R_{SG} was 0.81 at Xingan station (Ganjiang River) and 0.78 at Yichun station (Yuan River). Based on the above DEM data and the dynamic relationship between surface water level and groundwater level (Figure 3), we conclude that the channels of the Ganjiang River and Yuan River cut through the alluvial aquifer. The area enclosed by these water bodies is an independent hydrogeological unit surrounded with specific head boundaries. Rainfall is the main source of recharge of groundwater in the study area and it is then discharged to surface water for most of a hydrological year. However, surface water recharges groundwater between June and August when the surface water level rapidly increases with the increasing of inflow from upstream areas. Therefore, groundwater and river water exchange seasonally, groundwater flowing into rivers along the exposing aquifers in the dry and flat seasons and river water also recharging aquifers, replenishing the aquifer in the wet season.

METHODOLOGY

In order to identify the dynamic immersion process and make economic and scientific joint mitigation measures for controlling groundwater immersion, a groundwater numerical modeling based methodological framework was proposed, as shown in Figure 5. Firstly, we developed a three-dimensional groundwater flow model in the typical low-lying DFB of XGNPJ reservoir region. With regard to model reliability, the procedure of model calibration and sensitivity analysis were employed resulting in the

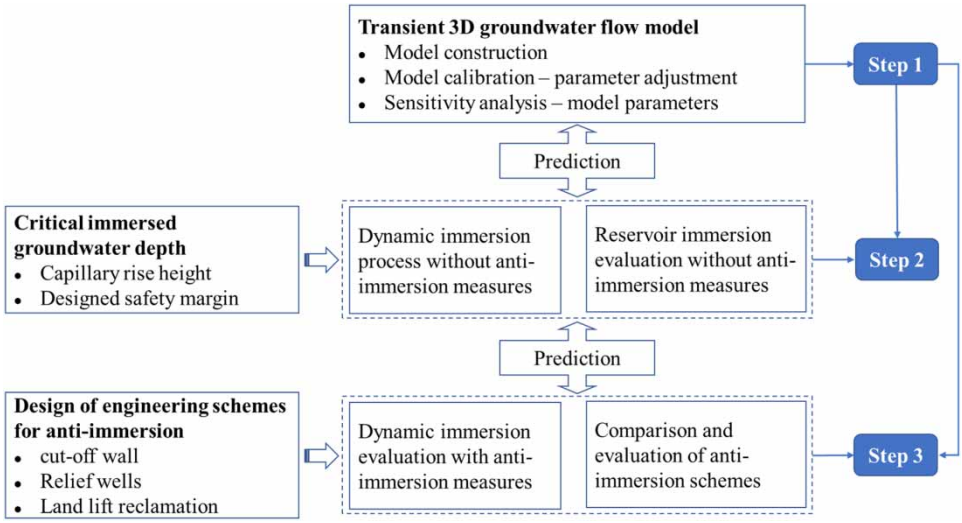

Figure 5 | Flowchart of reservoir immersion assessment and control based on numerical modelling.

determination of various aquifer parameters. Secondly, the calibrated transient model was used for prediction of the dynamic immersion process and reservoir immersion range without anti-immersion engineering measures based on the determination of the critical immersed groundwater depth. Thirdly, the effectiveness of the countermeasures adopted for the reduction of reservoir immersion areas were compared and analysed based on the simulation model by considering the projected future combination scenarios of engineering measures.

Groundwater model construction, calibration and sensitivity analysis

Basic mathematics for groundwater flow

To quantify the hydraulic interaction of groundwater with adjoining streams, we established a transient 3D groundwater flow model based on FEFLOW code (Diersch 2014). FEFLOW, combining GIS graphical features with finite element solution techniques, enables modeling of stream-aquifer systems in saturated and unsaturated porous media. The numerical solutions can be useful for determining aquifer hydraulic properties and predicting responses of aquifers to changing stream stage after reservoir impoundment. The governing partial differential equation describing the groundwater flow in a lower confined aquifer can be found in Diersch (2014) and Li *et al.* (2018). The water table in the upper leaky aquifer represents the upper free boundary of the three-dimensional groundwater flow system. The governing equation of groundwater flow in the upper unconfined aquifer with heterogeneity and anisotropy can be described as follows:

$$K_{xx}\left(\frac{\partial H}{\partial x}\right)^2 + K_{yy}\left(\frac{\partial H}{\partial y}\right)^2 - K_{zz}\frac{\partial H}{\partial z} + \varepsilon = \mu\frac{\partial H}{\partial t} \quad (x,\ y,\ z)\varepsilon\Gamma_1 \tag{1}$$

where K_{xx}, K_{yy}, K_{zz} are hydraulic conductivity along the x, y, z axis [L/T], H is the potentiometric head [L] at point (x, y, z), t is time [T], μ is specific yield [L^{-1}], ε is volumetric flux per unit volume [T^{-1}], Γ_1 is the free boundary of the water table.

Model setup

Based on stratigraphic records from 15 hydrogeological boreholes, the groundwater model consists of two aquifers and a bedrock basement (Figure 6). The upper aquifer (L1 and L2) is an unconfined and low-permeability layer comprising fill soil (L1) and underlying fine-grained sediments of silty clay (L2). The lower aquifer (L2 and L3) is a convertible confined aquifer composed of mostly alluvial materials of upper fine sand (L3) and lower medium-coarse sand and gravel (L4). The bedrock layer (L5) represents the bedrock

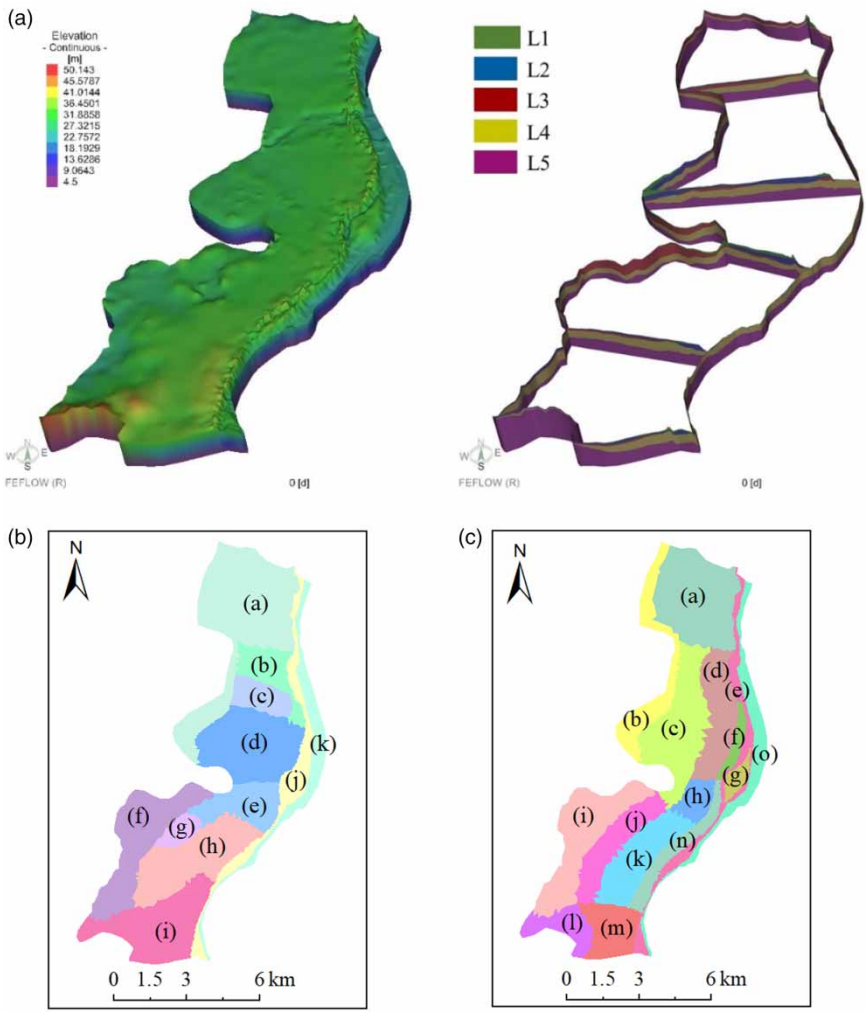

Figure 6 | The three-dimensional geological structure showing the topographic surface, internal geological profiles (a), and parameter zonation of net recharge rate in Layer L1 (b), and hydraulic conductivity, specific yield, specific storage in Layers L1-L4 (c).

formation of Yuqun Group, formed during the Tertiary and Cretaceous periods. The bedrock was treated as a weakly permeable layer as no apparent joints and fissures were found.

Each water-bearing layer (L1 and L2, and L3 and L4) was divided into 15 zones of hydrogeological parameters including hydraulic conductivity (K), specific yield (μ), and specific storage (S_s) (Figure 6(b)). The upper layer, L1, was divided into 11 zones of coefficient of recharge from precipitation (Figure 6(c)). In-situ survey parameters of K in L1-L4 layers, S_s in L3-L4 layers, collected from the pumping tests and slug tests, were used as the initial parameters before model calibration. The other initial value of relevant parameters of other layers shall be in accordance with the empirical value. The actual hydrogeological parameters for different zones were optimized from the model calibration described below.

The model domain was bounded by Ganjiang River and Yuan River (Figure 4), which were assigned as specified head boundary conditions. Constant heads along the river and lake boundaries were interpolated between monitored transient water levels recorded at Xingan and Yichun gauging stations (Jiangxi Hydrology Information Center for the period 1960–2014). The north and south boundaries (Line A-B, and Line D-E), the groundwater flow lines, should be set as no-flow boundaries. The model top was

assigned as flux boundary conditions representing groundwater recharge derived from precipitation infiltration. The fluxes were treated as a model calibration parameter of net recharge rate. The model bottom was assigned as a no-flow boundary condition, as the bedrock was simulated as the bottom layer.

Horizontally, the three-dimensional groundwater flow model was discretized into 63,239 triangular prismatic mesh elements with the lateral size of a mesh less than 200 m. Also, some meshes along river reaches were moderately refined to the lateral size ranging from 3 m to 40 m to delineate the topographic variation of river bed as accurately as possible. Vertically, the model extended from the ground surface to 80 m below sea level. The mesh was tested based on the Delunay criterion in order to avoid numerical problems. The flow time step, Δt, was set at a fixed number of 5 days during the period of model calibration from 1/1/2017 to 7/1/2017. The convergence criterion for the groundwater flow equation was 0.001 m.

Model calibration

We assume homogeneous and isotropic material property in each sub-domain as shown in Figure 6. Three fitting criteria including the root mean squared error (RMSE), the mean absolute error (MAE), and Nash-Sutcliffe coefficient of efficiency (NSE) were used to calibrate the numerical model.

$$\mathrm{RMSE} = \sqrt{\frac{\sum_{j=1}^{m}\sum_{i=1}^{n}(H_c^i - H_o^i)_j^2}{n}} \tag{2}$$

$$\mathrm{MAE} = \frac{\sum_{j=1}^{m}\sum_{i=1}^{n}|H_c^i - H_o^i|_j}{n} \tag{3}$$

$$\mathrm{NSE} = 1 - \frac{\sum_{j=1}^{m}\sum_{i=1}^{n}(H_c^i - H_o^i)_j^2}{\sum_{j=1}^{m}\sum_{i=1}^{n}(H_o^i - \overline{H_o^i})_j^2} \tag{4}$$

where H_c and H_o are the calculated head at jth time step from the simulation model and observed head at ith observation head targets, $\overline{H_o^i}$ is the mean of observed head, n is the number of observation locations, m is the number of time steps.

The calibration included two steps. Firstly, a steady state model was calibrated using the groundwater level in January 1th, 2017 to generate the initial conditions for the transient model. Besides, the material property and infiltration coefficient on the top layer of the model were initially adjusted. Secondly, the continuous groundwater level data from 1/1/2017 to 7/1/2017 was chosen to manipulate a transient state calibration. For all the transient simulation in this study, time step of the simulation was set to 5 days to meet the unstable variation driven by the surface water level fluctuation. After the transient calibration, the parameters of hydraulic conductivity (K), net infiltration rate, specific yield (μ), and specific storage (S_s) were adjusted to achieve a reasonable agreement between the simulated and measured groundwater levels. Scatter diagrams and hydrographs of simulated groundwater level against the observed value after transient calibration were shown in Figure 7.

The MAE and RMSE between the calculated and measured groundwater heads was 0.42 m and 0.1 m, respectively. 94.1% of the MAE values were less than 1.0 m, while 71.2% of the MAE values were less 0.6 m. The transient calculated groundwater level is consistent with the observed groundwater level during the calibration period, as shown in Figure 7(b). The NSE value of 0.92 was close to 1 indicating a good fit of transient series of simulated values to observed values. The overall calibration results indicate that the applied groundwater modeling can serve as a numerical tool for predicting the groundwater flow dynamics after normal operation of XGNPJ with reservoir impoundment and evaluating the effectiveness of implementation of countermeasures on controlling reservoir immersion. Therefore, the net recharge rate of the top layer and the hydraulic conductivity of the principal aquifers, which were improved (i.e., optimized) (Table 1) after model calibration, were implemented in the model assessment and prediction.

The observed data and calculated results highlight that both the surface water level and groundwater level showed obvious annual variation and the trends in their change were largely consistent, indicating that a close hydraulic connection exists between the main watercourses and the alluvial aquifer. Based on the relative elevations of stream stage and the groundwater head adjacent to the stream, groundwater

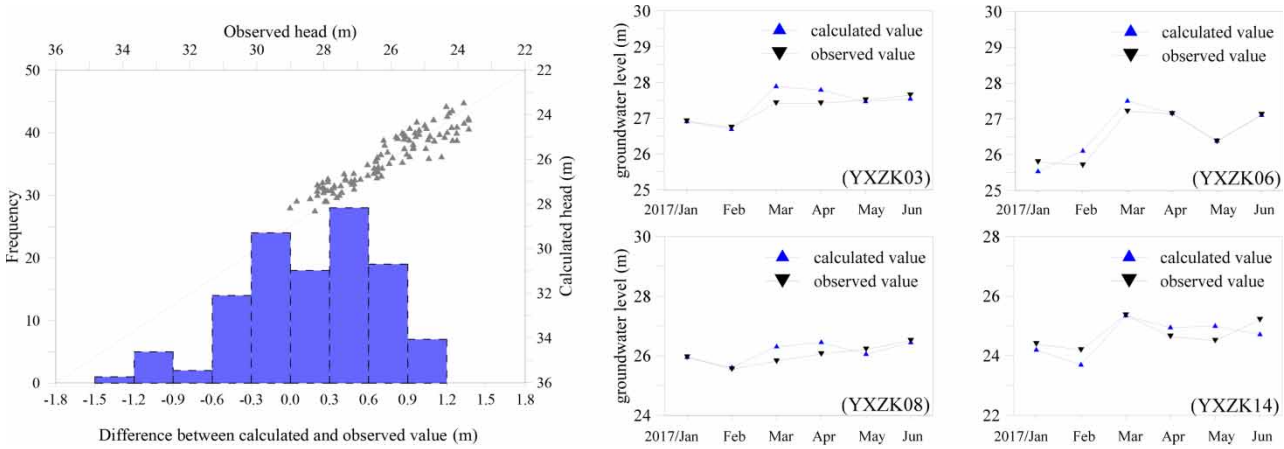

Figure 7 | Scatterplots and hydrographs of simulated vs. observed groundwater level based on transient model calibration.

Table 1 | Hydrogeological parameters of each layer in the study area after model calibration

	K/(m·d^{-1})					μ		S_s/m^{-1}			Net recharge rate
	L1	L2	L3	L4	L5	L1	L2	L3	L4	L5	L1
Value range	0.5 ~ 2.0	0.001 ~ 0.35	0.1~ 3.5	6.0~ 80.0	0.01	0.05 ~ 0.08	0.02 ~ 0.04	6.2×10^{-6} ~ 2.5×10^{-5}	6.2×10^{-6} ~ 1.2×10^{-5}	1.0×10^{-8}	0.003 ~ 0.078

mainly discharged to surface water bodies at the sites close to the rivers, while surface water recharged groundwater between June and July when the surface water level rapidly increases with the increasing of inflow from upstream areas.

Sensitive analysis

Sensitivity analysis (SA) was applied to vary model input parameters and evaluate how model results of groundwater flow dynamics change with these variations. In this study, the sensitivity of hydrogeological parameters including net infiltration rate, the specific yields of the L1 and L2 unconfined aquifers, the hydraulic conductivity and specific storage of L3 and L4 confined aquifers are analyzed to provide valuable understanding of both model implementation and the underlying physical processes, thus providing insight into model behavior. The relative sensitivity index (S_r) of the any parameter is estimated by using the following equation:

$$S_r = \left(\frac{1}{n'}\sum_{i=1}^{n'}\frac{|H_1^i - H_2^i|}{H_1^i}\right) / \left(\frac{|P_1 - P_2|}{P_1}\right) \quad (5)$$

In which, P_1 and P_2 are the possible low and high extreme parameter after model calibration, H_1^i and H_2^i are the corresponding model outputs in terms of the simulated target groundwater level at time i. The value of S_r is far from 0 indicates high sensitivity, and close to 0 indicates less sensitivity.

Sensitivity analysis was carried out on the net recharge coefficient from precipitation in sub-domains j and h (Figure 6(b)) and on the hydraulic conductivity, specific field and specific storage in sub-domains e and h (Figure 6(c)) for the year 2017 by changing the original hydrogeological parameters by the corresponding proportions as 20%, 50, 200 and 500%, respectively. Figure 8 shows the average S_r for the groundwater flow simulation model in the focused region. It is indicated that the model simulation results of groundwater level are most sensitive to the net recharge rate on the top layer, with an S_r of up to 0.7×10^{-3}. The groundwater flow dynamic is also relatively sensitive to the hydraulic conductivity of the sand-gravel layers (L3 and L4), with an S_r of up to 0.4×10^{-3}. In comparison, the simulation model was weakly sensitive to the parameters of

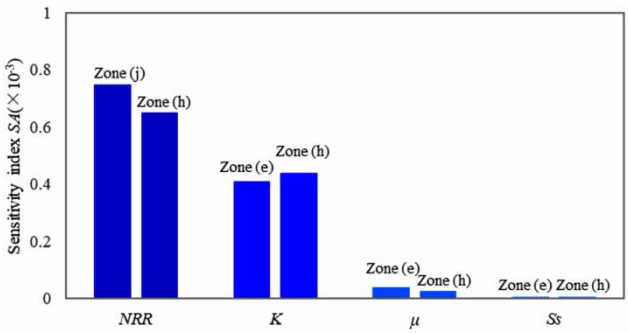

Figure 8 | Sensitivity index for the groundwater flow simulation model in the focused region (NRR = net recharge rate; K = hydraulic conductivity; μ = specific yield; S_s = specific storage).

specific field and specific storage. The error ratio between the calibrated and the field measured hydraulic conductivity by pumping tests and slug tests was calculated to be 1.46 m/d. To sum up, the properly characterizing net recharge rate on top layer L1 and hydraulic conductivity of Layers L3 and L4 and its interactions with other parameters provides improved prediction of transient aquifer responses, which can be used as the basis for the prediction of reservoir immersion of the left bank within the reservoir area of XGNPJ.

Critical immersed groundwater depth

Future influences of reservoir immersion need to be evaluated with respect to the positioning of the groundwater depth with critical immersed groundwater depth (GD_C), which is the evaluation criteria for reservoir immersion. When the groundwater depth is less than GD_C after the normal reservoir impoundment, it is deemed as the immersion area. The GD_C can be calculated according to the following formulation (Li *et al.* 2018):

$$GD_C = H_K + \Delta H \tag{6}$$

where, H_K is the height of capillary rise [L], and ΔH is the designed safety margin [L]. In this region, the extent of reservoir immersion can be broadly classified into two types, including slight immersion and high immersion with the ΔH of 1.5 m and 0.5 m, respectively. The capillary rise height can be defined as the distance from an obvious wet surface under the surface to the phreatic water level. According to the results of field experiment test, the height of capillary rise is 0.6 m in the study area. Therefore, the GD_C corresponding to the slight and high immersion is 1.1–2.1 m and <1.1 m, respectively.

Engineering measures for controlling reservoir immersion

The objective of this modeling study was to investigate how the combination of the engineering measures affects the groundwater system and the process of reservoir on the left bank of XGNPJ from 1/1/2018 to 1/1/2021. Therefore, to reasonably forecast the effects, we considered 8 schemes with different combinations of engineering countermeasures, including cut-off wall, relief wells, and land lift reclamation projects, as shown in Figure 9.

The cut-off wall constructed along the embankment are embedded below the bedrock surface, starting from the Dam Site A and ending at Node C, was divided into two sections. One is the section of high pressure jet grouting impervious wall from Dam Site A to Node B, and the other section is the water jetting anti-seepage wall from Node B to Node C. The thickness of high pressure jet grouting and water jetting

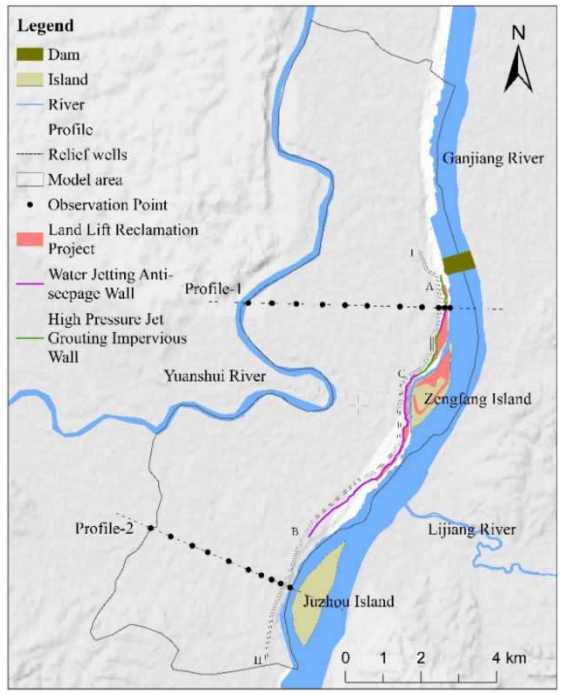

Figure 9 | Layout of engineering measures including cut-off walls, relief wells, and land lift reclamation for controlling reservoir immersion.

anti-seepage wall are 0.6 m and 0.2 m, and the designed K of both cut-off walls is 8.64×10^{-3} m/d. Considering the anti-seepage effect of the cut-off wall, the K of cut-off wall are assumed to be $1 \times 8.64 \times 10^{-3}$ m/d, $2 \times 8.64 \times 10^{-3}$ m/d, and $5 \times 8.64 \times 10^{-3}$ m/d in different controlling schemes. Relief wells drilled inside the embankment penetrated the sand gravel confined aquifers of layer L4, starting from Point I and ending at Point II, with the well spacing of 30 m. Relief wells are used to reduce pore water pressures in confined aquifers and permit the water level to be maintained below an elevation of the drainage level. Variable drainage levels of 29 m, 30 m, 31 m, and vertical distance from embankment of 30 m, 50 m, and 100 m are assumed for the relief wells in different countermeasures for reservoir immersion. In the reservoir regions outside the embankment, land lift reclamation projects are carried out in the low-lying farmland to prevent the farmland from being submerged. The 8 schemes are listed in Table 2, including Scheme S0 without any anti-immersion engineering measures, and Schemes S1-S7, the combination schemes with different K values of cut-off wall, and drainage level of relief wells and their vertical distance to the cut-off wall.

RESULTS AND DISCUSSION

Evaluation of the dynamic immersion process

Based on the 3D numerical model, the inside boundary conditions, such as the specified head boundary of Ganjiang River, were changed according to the process of SWI to predict the groundwater immersion process without any anti-immersion engineering measures. The surface water level after the normal operation of XGNPJ will be maintained at 32.5 m to meet the needs of navigation and power development. Taking January 1, 2018 as the start of the simulation, the calibrated groundwater model was used to predict the groundwater immersion process in the left bank of the reservoir over the next 3 years without any anti-immersion engineering measures (Scheme S0). Profile 1 with 11 observation points and Profile 2 with 13 observation points near the dam site were selected for analysis of groundwater dynamics (Figure 9), respectively. After SWI, groundwater level at 30 d, 100 d, 365 d, 730 d and 1,095 d in the upper unconfined aquifer (L1 and L2) and the lower confined aquifer (L3 and L4) were calculated as shown in Figure 10.

The dynamic changes in the groundwater level along the two profiles illustrate the groundwater immersion process along the reservoir bank with a dual-formation structure. The model results showed that after SWI, the confined water level increased continuously and quickly reached a stable state, as the river water had a close connection with the sand-gravel aquifer. The confined water table along two profiles formed a parabolic decrease from Ganjiang River (32.5 m) to Yuanhe River (24.2 m). The rapidly rising and maintaining high groundwater level in the confined aquifer exerted a vertical head pressure on the L1 and L2 unconfined aquifers throughout the upper boundary of the confined aquifer, causing the groundwater level of the upper unconfined aquifer to gradually rise. The numerical

Table 2 | Combination schemes of engineering measures for controlling reservoir immersion

		Relief well			
Schemes	**Hydraulic conductivity/(m/d)**	**Drainage level/m**	**Distance to cut-off wall/m**	**Well spacing/m**	**Land lift reclamation?**
S0	–	–	–	–	No
S1	$1 \times 8.64 \times 10^{-3}$	29	30	30	Yes
S2	$2 \times 8.64 \times 10^{-3}$	29	30	30	Yes
S3	$5 \times 8.64 \times 10^{-3}$	29	30	30	Yes
S4	$2 \times 8.64 \times 10^{-3}$	30	30	30	Yes
S5	$2 \times 8.64 \times 10^{-3}$	31	30	30	Yes
S6	$2 \times 8.64 \times 10^{-3}$	30	50	30	Yes
S7	$2 \times 8.64 \times 10^{-3}$	30	100	30	Yes

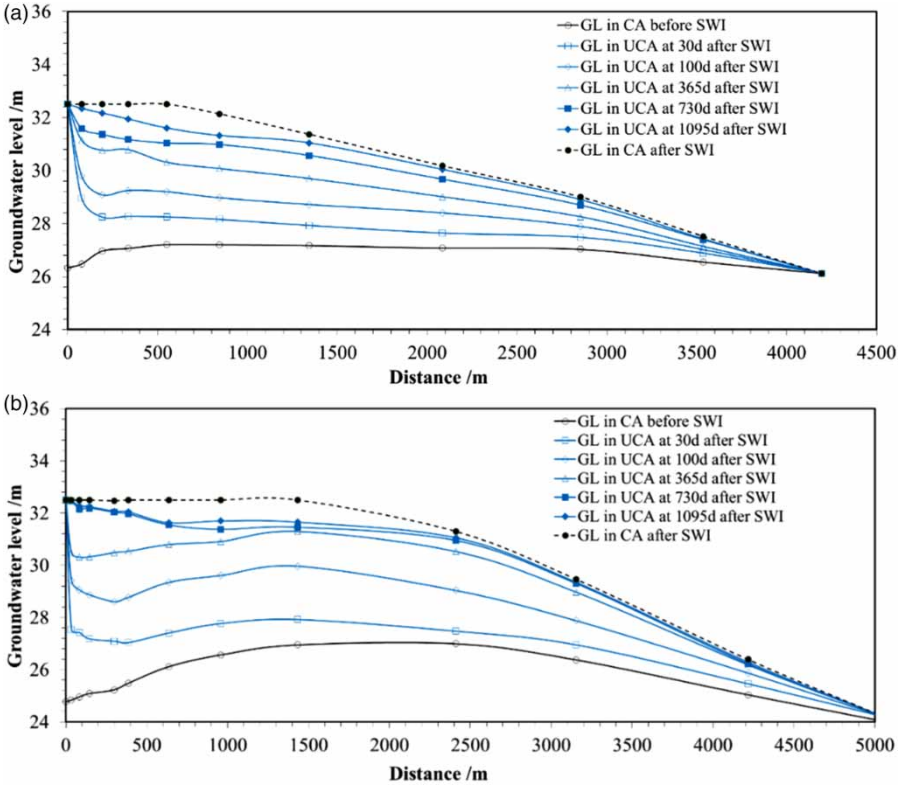

Figure 10 | Groundwater level variations at different times of (a) Profile 1 and (b) Profile 2 based on numerical solutions.

solution of the observation points at a distance of 80 m from the Ganjiang River in Profile 1 showed that in the unconfined aquifer the groundwater level increased with a rate of 0.037 m/d, from an initial water level of 26.5 m at 1/1/2018–27.5 m after 30 days. The unconfined water level increased to 29.9 m at 365 days, with a rate of increase of 0.0049 m/d. After 730 days, the unconfined water level rose to 30.5 m and the groundwater level stabilized. During the later stages, the unconfined water level increased at a lower rate of as little as 0.0011 m/d. The vertical head pressure in the confined aquifer to the upper unconfined aquifer decreases in the observation point at a distance of 1,340 m from the Ganjiang River showed that the increase rate of the unconfined groundwater level was lower than that in the riparian zone, with a rising rate of 0.02 m/d in the first 30 days. Subsequent to the water level remaining generally stable after two years, the increasing rate of groundwater in the unconfined aquifer was as low as 0.00055 m/d. As shown in Table 3, the dynamic immersion process calculated for Profile 2 was similar to that for Profile 1.

The simulation results show that during the early stage of SWI, the main driver of dynamic changes in groundwater in the upper unconfined aquifer was high head pressure in the lower confined aquifer, whereas the recharge from precipitation infiltration was the second-most influential factor. However, between the second year and the end of the third year, as the groundwater level increased in the unconfined aquifer, there is a decrease in the difference of groundwater level between lower and upper aquifers, resulting in a weakening hydraulic gradient from the lower confined aquifer. On the other hand, with the rise of groundwater level in the unconfined aquifer, the distance from surface infiltration recharge to the unconfined water table shortened, with some areas even becoming waterlogged. In addition, the results of the sensitivity analysis showed that the model was most sensitive to the net recharge coefficient of precipitation infiltration; therefore, the effect of rainfall infiltration recharge will gradually become the dominant factor driving groundwater immersion during the middle and later period. According to these results, the

Table 3 | Dynamic changes of groundwater level in calculation profiles after reservoir impoundment

	Profile 1						Profile 2					
Time (d)		Water table (m)	Rising rate (m/d)		Water table (m)	Rising rate (m/d)		Water table (m)	Rising rate (m/d)		Water table (m)	Rising rate (m/d)
0	80 m from Gan-jiang River	26.5	–	1340 m from Gan-jiang River	27.2	–	80 m from Gan-jiang River	25.0	–	1340 m from Gan-jiang River	27.0	–
30		27.6	0.037		27.8	0.020		26.6	0.053		28.1	0.037
100		28.6	0.014		28.6	0.011		28.4	0.026		29.7	0.023
365		29.9	0.0049		29.5	0.0034		30.2	0.0068		30.9	0.0045
730		30.5	0.0016		30.0	0.0014		30.9	0.0019		31.4	0.0014
1,095		30.9	0.0011		30.2	0.00055		31.2	0.00082		31.6	0.00055

well calibrated groundwater flow numerical model can accurately describe the dynamic process of reservoir immersion during different periods and can provide improved guidance for immersion control with pre-engineering optimization design.

Application of numerical model in reservoir immersion analysis

Based on the simulation model, the groundwater immersion range in reservoir region could be evaluated with and without any anti-immersion engineering measures. The model conditions can be adjusted with different K of cut-off walls, the location and drainage level of relief wells, and the range of land lift reclamation.

Reservoir immersion evaluation

1/1/2018 was taken as the initial time to predict groundwater immersion without any anti-immersion engineering measures (Scheme S0), and Figure 11 shows the range of slight and high immersion in the left bank of reservoir after three years of SWI. The simulation results showed a rapid advance of the groundwater flow into the embankment due to seepage immersion resulting from the uplift of the surface water level in the reservoir. Within the study

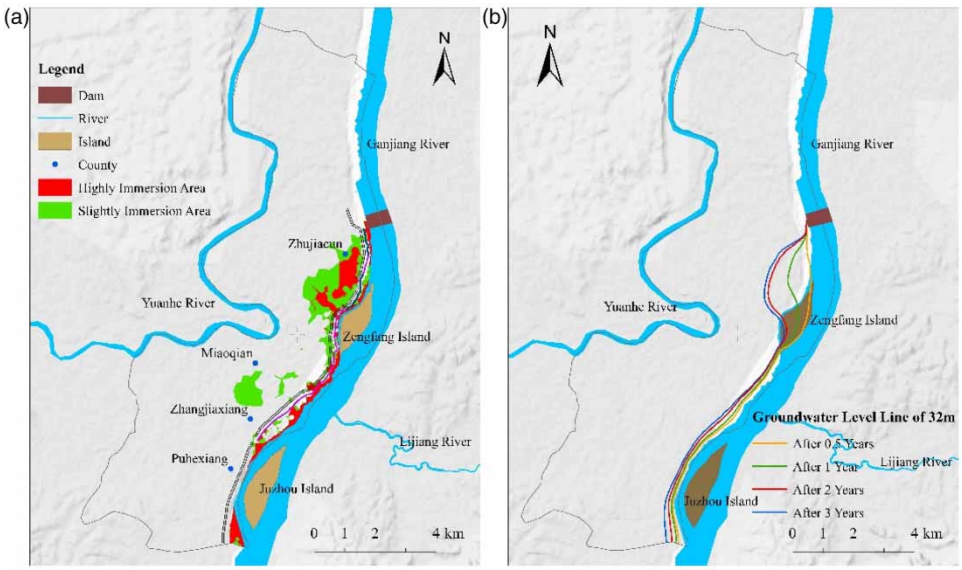

Figure 11 | Map of (a) immersion range and (b) groundwater level contour of 32 m under non-engineering scheme at different time.

area, the east part of Zengfang Island along the river terrace experienced the largest advance of the groundwater, whereas that of the south side of Hepu Town was the smallest. The immersion area was divided into two categories, namely the areas along the river and the area within the bank. The immersion area in the upper reaches of the Ganjiang River gradually weakened from the river side to the shore, especially for that in Zhujia Village near the upper reaches of the dam site. The immersion area within the bank was mainly located from Miaoqian Village to Zhangjiagang Village, and showed only slight immersion due to the low surface elevation.

The simulated groundwater level line of 32 m towards the reservoir bank at 0.5, 1, 2, and 3 years showed that the river was well connected to the groundwater, with the groundwater flow rapidly advancing into the embankment and the dynamics of groundwater flow changing from that under natural conditions. After two years of normal SWI, the groundwater flow remained generally stable. The groundwater level contour line of 32 m advanced 0.09 km–1.04 km into the embankment by the third year after SWI, with the reservoir immersion area gradually increased to 10.91 km^2.

Under Scheme S0, serious seepage immersion is predicted to occur along the left bank of the river and along low-lying areas within three years, with Table 4 showing the immersion area. The regional numerical groundwater flow model, as described in Section 3, was used in a comparative analysis of immersion control in the low-lying reservoir area under 7 combinations of engineering control measures, S1-S7 (Table 2), with the simulation results summarized in Table 4. Furthermore, Profile 1 and Profile 2 were selected to compare the groundwater level at selected points on the two profile lines under the different engineering control schemes, as illustrated in Figure 12.

Table 4 | Immersion area and groundwater drainage rate from relief wells under different engineering measures

Schemes	Area of high immersion/ km^2	Area of slight immersion/ km^2	Total area of reservoir immersion/km^2	Water drainage rate/(m^3/d)
S0	4.000	6.930	10.910	\
S1	1.571	2.724	4.295	85,376
S2	1.551	2.615	4.166	102,066
S3	1.539	2.567	4.106	115,461
S4	1.626	2.654	4.863	82,853
S5	2.077	5.596	7.673	56,294
S6	1.760	3.131	4.891	77,344
S7	1.773	3.178	4.951	77,180

Analysis of engineering measures on groundwater immersion control

Under the control schemes S1–S3, while the surface water in the reservoir river slowly advanced into the embankment after SWI, and the groundwater level inside the embankment could be controlled to remain below 30 m (Figure 13), with the immersion area in the study area reduced by about 60% compared to that under Scheme S0. Under the constant drainage level (29 m), well spacing (30 m), and distance to the cut-off wall (30 m) of the relief wells, with a decrease in the hydraulic conductivity of the cut-off wall, the total immersion area almost remains

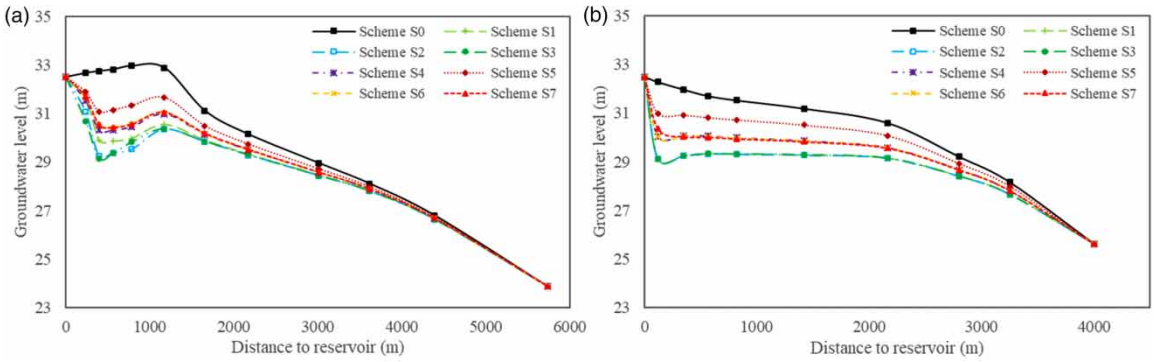

Figure 12 | Comparison of groundwater levels in Profile 1 (a) and Profile 2 (b) under different engineering measures.

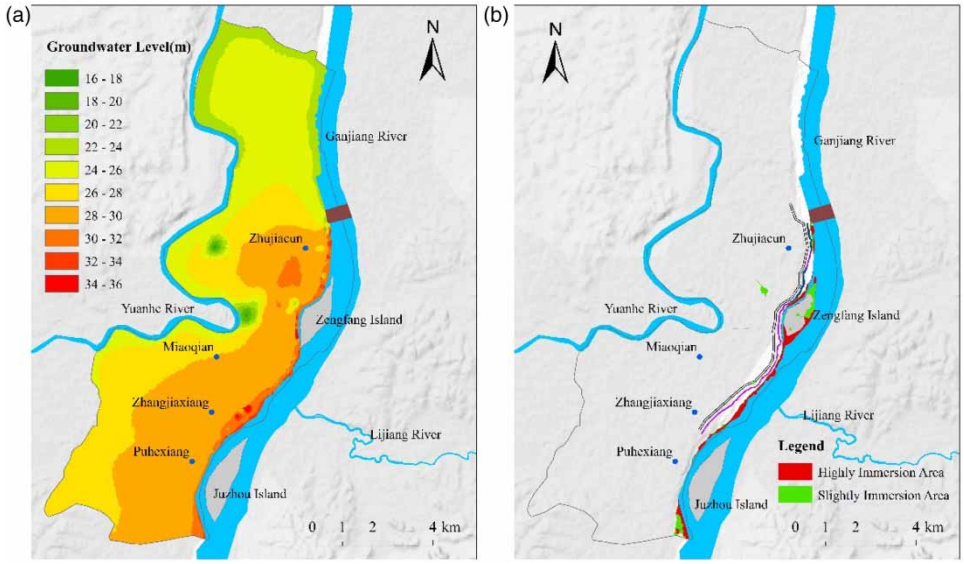

Figure 13 | Groundwater flow (a) and immersion area (b) after three years' SWI under scheme S2.

unchanged, while the total water drainage rate decreased from 115,461, 102,066, to 85,376 m^3/d, mainly because the cut-off wall slowed down the discharge of rising groundwater level from the area outside the embankment to the inside area. For the selected points outside the embankment in Profile 1 crossing the impervious area, the groundwater level under Scheme S1 was higher than that under S2 and S3, while for Profile 2 crossing the non-impervious area, the groundwater level under schemes S1–S3 were similar because the drainage levels of the relief wells remained the same under the three schemes.

Under control schemes S2, S4, and S5, different drainage levels were set under the condition that the K of the cut-off wall, well spacing and distance to the cutoff wall from relief wells remained unchanged. With an increase in the drainage level, the immersion areas under S4 and S5 expanded continuously after SWI, although the total water drainage rate decreased from 102,066, 82,853, to 56,294 m^3/d. The groundwater levels at selected points inside and outside the embankment on Profiles 1 and 2 also increased with large variations, indicating that the drainage level in relief wells is an important parameter for reservoir immersion in the case of the construction of the cut-off wall.

Under schemes S4, S6 and S7, different distances of 30 m, 50 m and 100 m from relief wells to the cut-off wall were set under unchanged hydraulic conductivity of cut-off wall, drainage level and well spacing of relief wells. After SWI, the immersion area increased slightly with increased distance between the relief wells and cut-off walls, while the total water drainage rate decreased from 82,853, 77,344, to 77,180 m^3/d. The groundwater levels of selected points inside and outside the upper embankment on Profiles 1 and 2 were similar, with little overall variation.

To sum up, in order to reduce the unfavorable influence of SWI on the agriculture and residential life on the bank of the reservoir, appropriate measures should be taken to reduce the groundwater level inside the cut-off wall and to reduce the thickness of the capillary saturation zone using relief wells in order to achieve effective protection. An anti-seepage wall can easily block the rapid seepage of groundwater; however, it breaks the original nature exchange between surface water and groundwater in the riparian zone. Especially in the wettest season, the rising groundwater inside the embankment recharged from precipitation is difficult to discharge to the river, which leads to the groundwater inundation. For the dualistic structure stratum, relief wells can be used not far away from the dike and can greatly reduce the water table and reduce the pressure head at the bottom of the impermeable layer for the purpose of immersion control. The drainage level of the relied well is the most important parameter for immersion control, which

directly affects the immersion area and drainage rate. Therefore, aiming at the phenomenon that the water storage of XGNPJ leads to a high groundwater level on the left bank of the reservoir, it is suggested to arrange the joint countermeasures of Scenario S2 with a cut-off wall and relief wells along the axis of the auxiliary dam, in which the hydraulic conductivity of the cut-off wall is less than 17.28×10^{-3} m/d; the drainage water level of relief wells is 29 m, to alleviate the immersion of the XGNPJ reservoir bank.

CONCLUSIONS

The surface water impoundment (SWI)-driven groundwater immersion in the reservoir region is expected to be a serious environmental geological issue in a dual-formation structural reservoir bank. Aiming to deal with this issue, a three-dimensional (3D) groundwater model was established for reservoir immersion evaluation and control in the downstream area of the left bank of XGNPJ.

(1) The results of model calibration and sensitivity analysis indicate that the net recharge coefficient is most sensitive to groundwater flow dynamics, and a better fit of simulated values to targets is obtained, which can be used as a numerical tool for prediction of groundwater immersion in the plain reservoir area.
(2) Based on the 3D groundwater flow model, groundwater immersion under the effect of SWI was evaluated without any anti-seepage measures (S0). By the end of the third year of SWI, the 32 m groundwater level contour advanced 0.09–1.04 km into the embankment region, and the immersion area gradually increased to 10.91 km^2. It can be expected that the actual extent of reservoir immersion in the future would be more severe than the model prediction. Better strategies for controlling groundwater inundation and scheme comparison will be necessary to choose optimal countermeasures to protect the adjunct aquifers from immersion by SWI.
(3) The joint engineering countermeasures, including the cut-off wall, relief wells, and land lift reclamation projects can effectively control reservoir immersion. With the construction of the cut-off wall, the drainage water level of the relief well is the most sensitive parameter for controlling reservoir immersion, while the hydraulic conductivity of the cut-off wall and the distance between the relief well and cut-off wall are the secondary sensitive parameters. According to the comprehensive comparative analysis, it is suggested that the joint immersion control engineering measures should be set as follows: the hydraulic conductivity of the cut-off wall is less than 17.28×10^{-3} m/d; the drainage water level of relief wells is 29 m; the relief well spacing is 30 m; the vertical distance between the relief wells to the cut-off wall is 30 m; and the elevation of land lifting reclamation outside the embankment is more than 33 m.

ACKNOWLEDGEMENTS

This work was partially supported by the National Key R&D Program of China (No. 2019YFC1804304), the Fundamental Research Funds for the Central Universities (No. B200202014), the Science and Technology Project of Department of Transportation, Jiangxi Province (No. 2016C0053), and the National Natural Science Foundation of China (No. 41572209).

DATA AVAILABILITY STATEMENT

All relevant data are included in the paper or its Supplementary Information.

REFERENCES

Azamathulla, H. M., Wu, F. C., Ghani, A. A., Narulkar, S., Zakaria, N. A. & Chang, C. K. 2008 Comparison between genetic algorithm and linear programming approach for real time operation. *Journal of Hydro-Environment Research* **2** (3), 171–180.

Cao, H., Sun, Z. J., Li, J. & Fu, N. J. 2009 Prediction and monitoring analysis of immersion effects of Chaozhou City Zone. *Chinese Journal of Rock Mechanics and Engineering* **28** (11), 2161–2166.

Chen, D. M., Liu, H. W., Lu, W. X., Gong, L. & Zhang, Q. 2016 Calculation of seepage under the effect of a suspended anti-seepage wall in the heterogeneous formation, exemplified by

the Qunli Dam in the Songhua River. *Hydrogeology & Engineering Geology* **43** (4), 14–19.

Chen, J., Huang, Y., Yang, Y. M. & Wang, J. J. 2018 Evaluation of the influence of Jiangxiang Reservoir immersion on crop and residential areas. *Geofluids* **2018**, 9720970. https://doi.org/10.1155/2018/9720970.

Diersch, H. J. G. 2014 *FEFLOW: Finite Element Modeling of Flow, Mass and Heat Transport in Porous and Fractured Media*. https://doi.org/10.1007/978-3-642-38739-5.

Dos Santos, J. S., De Oliveira, E., Bruns, R. E. & Gennari, R. F. 2004 Evaluation of the salt accumulation process during inundation in water resource of Contas river basin (Bahia-Brazil) applying principal component analysis. *Water Research* **38** (6), 1579–1585.

Fowler, D. K. & Maddox, J. B. 1974 Habitat improvement along reservoir inundation zones by barge hydroseeding. *Journal of Soil &Water Conservation* **29** (6), 263–265.

Guo, Y. Z. & Chen, L. S. 2008 *Investigation Report on Groundwater Resources in Poyang Lake Basin, Jiangxi Province,* Jiangxi Geology & Mineral Exploration Bureau Report No. 0900324852.

Guo, Q. N., Zhou, Z. F., Huang, G. J. & Dou, Z. 2019 Variations of groundwater quality in the multi-layered aquifer system near the Luanhe River, China. *Sustainability* **11** (4), 994.

Habel, S., Fletcher, C. H., Rotzoll, K. & El-Kadi, A. I. 2017 Development of a model to simulate groundwater inundation induced by sea-level rise and high tides in Honolulu, Hawaii. *Water Research* **114**, 112–134.

Hao, H. K., Zhan, M. L., Sheng, J. C. & Luo, Y. L. 2011 Optimizing saturated and unsaturated seepage of raising farmland based on multi-component three-dimensional finite element analysis. *Bulletin of Soil and Water Conservation* **31** (5), 259–262.

Hu, G. C., Liang, X., Pan, H. Y. & Liu, L. Y. 2015 Comparison of calculation method for the banked-up water level of double-layer structural terrace in the immersion evaluation. *Bulletin of Geological Science and Technology* **34** (1), 191–197.

Jia, J. S. 2016 A technical review of hydro-project development in China. *Engineering* **2** (3), 302–312.

КАМЕНСКИЙ, ГН. 1995 *Principle of Groundwater Dynamics*. Geological Processes, Beijing, China.

Li, M. Y., Zhou, Z. F., Yang, Y., Xin, Y., Liu, Y., Guo, S. G., Zhu, Y. & Jin, D. 2018 Immersion assessment and control of the right bank of Xingan navigation and power junction. *Journal of Hohai University (Nature Sciences)* **46**, 203–210.

Liu, J. G., Zhang, C. F., Tian, S. Y., Yang, H., Jia, S. Y., You, L. Z., Liu, B. & Zhang, M. 2013 Water conservancy projects in China: achievements, challenges and way forward. *Global Environmental Change* **23**, 633–643.

Liu, Y. N., Zhou, Z. F., Yang, Y. & Li, M. Y. 2018 Prediction and control of groundwater immersion of the mid-channel bar. *Hydro-Science and Engineering* **6**, 62–69.

Luo, Z. J., Yang, L., Li, Z. & Wang, J. 2012 Three-dimensional numerical simulation for immersion prediction of left bank of Songyuan reservoir project. *Transactions of the Chinese Society of Agricultural Engineering* **28**, 129–134.

Mahdavi, A. 2015 Transient-state analytical solution for groundwater recharge in anisotropic sloping aquifer. *Water Resources Management* **29**, 3735–3748.

Qin, Y. & Zhang, L. J. 2010 Evaluation on reservoir immersion in Songbei district of Harbin. *Journal of Jilin University (Earth Science Edition)* **40** (1), 134–139.

Shu, L. C. & Chen, X. H. 2002 Simulation of water quantity exchange between groundwater and the Platte River water, central Nebraska. *Journal of Central South University* **40** (5), 918–924.

SRTM Data. Shuttle Radar Topography Mission (SRTM), US Geological Survey. Available from: https://srtm.csi.cgiar.org/srtmdata/

Wang, J. M. & Liu, H. N. 2011 Seepage control of unsaturated soil based on the SWCC. *Hydrogeology & Engineering Geology* **38** (5), 115–119.

Wang, X. Y., Dang, F. N., Tian, W., Zhang, J. Y. & Xiao, Y. T. 2008 Determination of depth of suspended cut-off walls in cofferdam of a hydraulic power station in Dadu River. *Chinese Journal of Geotechnical Engineering* **30** (10), 1564–1568.

Wu, C. Y., Li, S. S. & Zhang, W. 2001 Research on effects of underground water to immersion at urban area of Laohekou city by analytic element method. *Journal of Yangtze River Scientific Research Institute* **18** (5), 61–63.

Xin, Y. W., Zhou, Z. F., Li, M. W. & Zhuang, C. 2020 Analytical solutions for unsteady groundwater flow in an unconfined aquifer under complex boundary conditions. *Water* **12** (1), 75. https://doi.org/10.3390/w12010075.

Yan, F., Tu, X. B. & Li, G. 2004 The uplift mechanism of the rock masses around the Jiangya dam after reservoir inundation, China. *Engineering Geology* **76** (1–2), 141–154.

Yin, Q. H. & Lu, Z. G. 2015 Immersion treatment of the protection engineering for reservoir region of Shihutang Navigation-power Project in Ganjiang River. *Jiangxi Hydraulic Science & Technology* **5**, 383–386.

Yin, J. B., Guo, S. L., He, S. K., Guo, J. L., Hong, X. J. & Liu, Z. J. 2018 A copula-based analysis of projected climate changes to bivariate flood quantiles. *Journal of Hydrology* **566**, 23–42.

Zhang, Y. Q., You, Q. L., Chen, C. C. & Li, X. 2017 Flash droughts in a typical humid and subtropical basin: a case study in the Gan River Basin, China. *Journal of Hydrology* **551**, 162–176.

First received 25 November 2020; accepted in revised form 7 February 2021. Available online 18 February 2021